Photobio-electrocatalytic production of H2 using fluorine-doped tin oxide (FTO) electrodes covered with a NiO-In2S3 p-n junction and NiFeSe hydrogenase

Gabriel Luna-López, Melisa del Barrio, Jennifer Fize, Vincent Artero, Ana Margarida Coito, Inês A.C. Pereira, José Carlos Conesa, Ana Iglesias-Juez, Antonio L. de Lacey, Marcos Pita

Bioelectrochemistry 150 (2023) 108361

Contents lists available at ScienceDirect

Bioelectrochemistry

journal homepage: www.journals.elsevier.com/bioelectrochemistry

Photobio-electrocatalytic production of H_2 using fluorine-doped tin oxide (FTO) electrodes covered with a NiO-In_2S_3 p-n junction and NiFeSe hydrogenase

Gabriel Luna-López [a], Melisa del Barrio [a,b], Jennifer Fize [c], Vincent Artero [c], Ana Margarida Coito [d], Inês A. C. Pereira [d], José Carlos Conesa [a], Ana Iglesias-Juez [a], Antonio L. De Lacey [a], Marcos Pita [a,*]

[a] Instituto de Catálisis y Petroleoquímica, CSIC, c/Marie Curie 2, 28049 Madrid, Spain
[b] Departamento de Química Analítica y Análisis Instrumental, Universidad Autónoma de Madrid, Campus de Cantoblanco, Madrid 28049, Spain
[c] Univ Grenoble Alpes, CNRS, CEA, IRIG, Laboratoire de Chimie et Biologie des Métaux, 38000 Grenoble, France
[d] Instituto de Tecnologia Química e Biológica António Xavier, Universidade Nova de Lisboa, 2780-157 Oeiras, Portugal

ARTICLE INFO

Keywords:
Photocatalysis
Biocatalysis
Hydrogenase
Nickel oxide
Indium sulfide
Hydrogen

ABSTRACT

Clean energy vectors are needed towards a fossil fuel-free society, diminishing both greenhouse effect and pollution. Electrochemical water splitting is a clean route to obtain green hydrogen, the cleanest fuel; although efficient electrocatalysts are required to avoid high overpotentials in this process. The combination of inorganic semiconductors with biocatalysts for photoelectrochemical H_2 production is an alternative approach to overcome this challenge. *N*-type semiconductors can be coupled to a co-catalyst for H_2 production in the presence of a sacrificial electron donor in solution, but the replacement of the latter with an electrode is a challenge. In this work we attach a NiFeSe-hydrogenase with high activity for H_2 production with the *n*-type semiconductor indium sulfide, which upon visible irradiation is able to transfer its excited electrons to the enzyme. In order to enhance the transfer of the generated holes towards the electrode for their replenishment, we have explored the inclusion of a p-type material, NiO, to induce a p-n junction for H_2 production in a photoelectrochemical biocatalytic system in absence of sacrificial reagents.

1. Introduction

In the last decades the greenhouse effect, climate change and global warming have risen as top challenges to face and solve for humanity. Global environmental policies have been designed and science is committed to deliver solutions. The use of fossil fuels has increased atmospheric carbon dioxide to levels higher than 410 ppm, which doubles the pre-industrial levels and threatens the environment. Currently most of the energy consumption is still dependent on fossil fuels and renewable energy sources need more alternatives and support from non-polluting energy technologies. A large part of scientists in the field have looked to nature for inspiration, developing new ways to accomplish artificial photosynthesis and bring together sunlight energy harvesting with electricity production or even chemical synthesis [1 2]. One of the top-tier fuels is hydrogen: H_2 is the most energetic single bond known, protons are the prime matter to produce it, which are very abundant and its oxidation yields only water, which has no polluting effect at all. Currently, more than 90 % of the H_2 available is produced in industrial plants from hydrocarbons, meaning that even using fuel cells able to work with H_2 the carbon footprint is still very high [3]. Sustainable synthetic routes that avoid hydrocarbons are needed for a real impact of hydrogen economy.

Besides hydrocarbons, another proton source to produce H_2 is water. Upon energy application, it is possible to dissociate it into H_2 and O_2, also called water splitting. There are several ways to provide the energy, yielding electrolysis or photolysis among other processes. A key aspect is that the energy needed in this process should be much higher than the 1.23 eV required by thermodynamics to overcome both the endothermic cooling of the reaction and the overpotentials inherent to energy activation processes. Therefore, catalysts are needed to lower the activation energy and speed the reaction. The first inorganic photocatalyst reported for simultaneous hydrogen and oxygen production from water

This article is for the Evgeny Katz's 70th anniversary special issue.

* Corresponding author.

https://doi.org/10.1016/j.bioelechem.2022.108361
Received 26 October 2022; Received in revised form 27 December 2022; Accepted 28 December 2022
Available online 30 December 2022

splitting was TiO_2 [4], which used ultraviolet radiation to accomplish the reaction. Since then, many works have blossomed in this field [5] studying the different TiO_2 crystalline structures, combining the material with either doping elements [6] or molecular dyes as sensitizers [7] to lower the bandgap, or using co-catalysts to improve its activity [8]. TiO_2 is not the only semiconductor able to split water, a panoply of examples has been investigated in the last decades, opening the field for many different applications and processes. Besides inorganic catalysts for H_2 production there are enzymes known as hydrogenases (Hases) performing this reaction reversibly in living organisms such as cyanobacteria or some plants. Hases have been a matter of research for several decades and present advantages like working at standard temperature and pressure in aqueous solutions [9,10]. The inherent dipolar moment on the protein structure surface of some hydrogenase allows their oriented immobilization on tailored electrodes to successfully achieve direct electron transfer [11]. Hases also perform mediated electrocatalysis with low potential redox polymers like those based on viologens, which were a matter of joint research by Professor Evgeny Katz and Professor Victor M. Fernandez in the early 90′s during a secondment in Madrid, Spain [12,13].

Semiconductors based on sulphides are promising alternatives to TiO_2 as some of them present visible band-gap, which makes them suitable to harvest the most abundant radiation coming from the Sun to Earth. Also, quantum dots made of CdS, CdSe have been demonstrated as a suitable alternative to host hydrogenases and facilitate its biological activity upon irradiation [14]. Other sulphides may be studied, looking particularly at their properties. Not only a suitable bandgap able to harvest photons in the visible energy range is needed, but also the energy level of the excited electrons is mandatory to be high enough to directly produce the proton reduction or transfer electrons to a co-catalyst where the reaction occurs. Indium sulphide, In_2S_3, fulfills these requirements and can work together with an enzymatic co-catalyst like hydrogenase (Hase) to produce H_2 from water upon visible light irradiation in solution, using a sacrificial electron donor [15]. However, a limitation for In_2S_3 appears when the sacrificial electron donor is replaced with an electrode, aiming to supply electrical power instead of chemical power. As In_2S_3 is an *n*-type semiconductor it barely transfers holes to the electrode, whereas it does transfer excited electrons. This implies that under this configuration electrode-assisted oxidative processes are favored, as it has been shown for oxygen evolution catalyzed by laccase on FTO-In_2S_3 electrodes [16] or FTO-SnS_2 electrodes [17].

Another approach to use In_2S_3 for electrochemical H_2 production from water is to deposit it on an electrode previously modified with a suitable p-type semiconductor, building a p-n junction that would favor charge separation, pumping holes to the electrode surface. p-n junctions have already been reported for other bio-related applications like tumor therapy [18], glucose biosensors [19,20] or pollutants detection [21]. These previous reports unveil the possibility of producing H_2 by feeding hydrogenase with high energy electrons originated by a p-n junction irradiation, allowing the holes' replenishment by the cathode at low or no overpotential at all. In the present work we explore this photo-bioelectrode concept using FTO as electrochemical supporting material, NiO as p-type semiconductor, In_2S_3 as *n*-type semiconductor and *DvH* NiFeSe-hydrogenase (Hase) as enzymatic co-catalyst for photoproduction of H_2, Scheme 1.

2. Materials & methods

2.1. Reagents and materials

$InCl_3$ 99.999 %, thiourea 99 %, 4-morpholineethanesulfonic acid (MES hydrate) 99.5 %, fluorine-doped tin oxide (FTO) coated glass slides, tris(hydroxymethyl)-aminoethane (TRIS) 99 %, 1-ethyl-3-(3-dimethylaminopropyl) carbodiimide (EDC) 99 %, BF_4NBu_4 99 %, p-nitrophenyldiazonium tetrafluoroborate 97 %, nickel (II) nitrate hexahydrate 98.5 % were purchased from Sigma-Aldrich. Ethanol absolute (EtOH) 99.5 %, acetone 99.5 %, acetonitrile and ethylenediamine 98 % were acquired from Scharlau. *N*-hydrosuccinimide (NHS) 97 % was purchased from Fluka. HCl 37 %, disodium hydrogen phosphate 12-hydrated 99 %, ethylene glycol 98 %, potassium chloride 99 %, sodium chloride 98 %, sodium dihydrogen phosphate dihydrate 99 % were obtained from Panreac. Acetonitrile 99,99 % was purchased from VWR Chemicals. Technical dielectric paste was purchased to SunChemical. All water solutions were elaborated with MilliQ deionized water (18.2 MΩ·cm).

2.2. Purification of Desulfovibrio vulgaris Hildenborough [NiFeSe] hydrogenase (Hase)

The [NiFeSe] hydrogenase used in this work was the recombinant soluble form purified from the organism *Desulfovibrio vulgaris Hildenborough*, according to a previous report [22]. The molecular weight of the Hase is 85 kDa.

2.3. Synthesis of In_2S_3

A hydrothermal procedure was used to synthesize the polycrystalline powder of In_2S_3 [23].

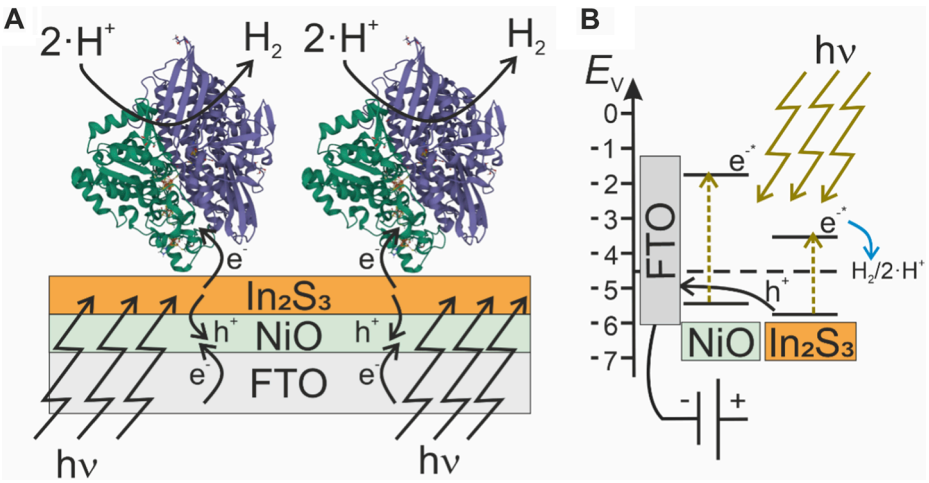

Scheme 1. (A) FTO electrode modified layer-by-layer with NiO and In_2S_3 to produce a p-n junction suitable to pump excited electrons to Hase co-catalyst and holes to the FTO electrode. (B) Transport of electrons and holes upon visible irradiation represented on the absolute energy diagram schematics of the semiconductors deposited on the FTO electrode.

2.4. Preparation of FTO-NiO electrodes

The coverage of FTO electrodes with NiO was performed adapting a known procedure used for indium tin oxide (ITO) electrodes [24]. FTO slides were used as substrate to grow a nickel oxide (NiO) layer on top of it. To carry out this modification, an ethylene glycol solution containing 1 M $Ni(NO_3)_2$ and 1 M ethylenediamine was prepared. Then, 100 μL of this solution was deposited by spin coating onto the electrode while spinning at 5,000 rpm, increasing to 6,000 rpm for 45 s later. The electrode was then treated thermally as follows: first, the electrode went through a 2 °C/min ramp up to 100 °C, then it was kept at a sustained 100 °C temperature for 40 min, finally the electrode went through a second 2 °C/min ramp up to 300 °C, to which it was kept for 1 h. A total of three successive layers were deposited on the electrode. The homogeneity of the surface was checked by Scanning Electron Microscopy (SEM). A metallic wire was attached with adhesive conducting tape to one extreme of the FTO-NiO slide and the electrodes were then masked with dielectric paste, to let only a window of 0.27 cm^2.

2.5. Preparation of FTO-NiO-In_2S_3 photoelectrodes

A 12 $mg{\cdot}mL^{-1}$ In_2S_3 dispersion in CH_3CN was prepared by immersion in an ultrasonic bath during 15 min. This dispersion was used immediately for its deposition on the FTO-NiO electrodes by spin coating as follows: 35 μL of the In_2S_3 suspension in acetonitrile was laid on a FTO-NiO slide while it spun at 5,000 rpm. After 30 s, the rotation speed was increased to 6,000 rpm during 45 s. The prepared electrodes were then subjected to a thermal treatment of 150 °C for 10 min to evaporate the solvent. The spin coating process was repeated several times. The number of final layers corresponded to the optimal photoelectrochemical performance found. Finally, a metallic wire was attached to the modified slide and after masked as in the case of FTO-NiO electrodes.

2.6. Modification of FTO-NiO-In_2S_3 photoelectrodes with adsorbed Hase

For the immobilization of Hase by adsorption, the enzyme is diluted in 10 mM MES buffer at pH 6, to reach a Hase concentration of 8.21 μM. 18 μL were then deposited onto the electrode and covered for 30 min so that the solution did not dry. If required, additional 6 μL of MES pH 6 buffer were added to avoid complete drought. After 30 min incubation, the electrode was set into the electrocatalytic cell.

2.7. Oriented covalent immobilization of Hase to FTO-NiO-In_2S_3 photoelectrodes

For the oriented covalent immobilization of Hase, the electrode was first functionalized with 4-nitrophenyl diazonium (NBD) salt. The FTO-NiO-In_2S_3 electrode was placed in a solution of 2 mM NBD, 0.1 M BF_4NBu_4 in $CNCH_3$, and was subjected to 2 cyclic voltammograms with a range from 0.8 V to 0.1 V and a rate of 100 $mV{\cdot}s^{-1}$. This first step set a layer of nitrobenzyl derivatives on the surface of the electrode [25]. The electrode was rinsed with deionized water before the second modification step, in which another 2 cyclic voltammograms were applied at 100 $mV{\cdot}\ s^{-1}$ in the range from 0.2 V to −1.2 V in a solution of 0.1 M KCl in 1:9 EtOH/H_2O. This step reduces the nitro group of the 4-nitrophenyl to an amine group [25]. 18 μL of 8.21 μM Hase in 10 mM MES pH 6 were then deposited on the electrode surface and left to incubate for 30 min. After that, 18 μL of a solution of 9.45 mM NHS and 7.7 mM EDC was deposited on the electrode and left to incubate for 90 min for formation of amide bonds between the amino groups of the electrode surface and carboxylic groups of the Hase. If required, additional 6 μL of the MES pH = 6 buffer were added to keep the electrode moist. After this last incubation, the electrode was gently rinsed with buffer solution before being put into the electrochemical cell.

2.8. Preparation of FTO-In_2S_3 photoelectrodes

The FTO-In_2S_3 photoelectrodes were prepared following the same spin-coating deposition procedure already described for preparing FTO-NiO-In_2S_3 electrodes but using clean FTO substrate.

2.9. Preparation of FTO-In_2S_3-Hase photoelectrodes

The FTO-In_2S_3-Hase photoelectrodes were prepared following the same absorption modification procedure already described for preparing FTO-NiO-In_2S_3 electrodes but using FTO-In_2S_3 as substrate.

2.10. Electrochemical measurements

The electrochemical characterization was carried out in a 3-electrode cell controlled by a μ-Autolab Type III with Nova 1.0 software. Unless otherwise stated, the reference electrode was a BAS Ag/AgCl (3 M NaCl) electrode and a platinum wire was used as counter electrode. The techniques used were cyclic voltammetry, chronoamperometry and electrochemical impedance spectroscopy, connected to a 150 W Xe solar simulator (Quantum Lot) tuned to simulate 1 sun irradiation power. Measurements were taken under both, dark and light conditions.

2.11. X-ray photoemission spectroscopy

In_2S_3 was characterized by X-ray Photoemission Spectroscopy (XPS) in two configurations, first as a pressed pellet and second after its deposition on the FTO-NiO-In_2S_3 electrode. The sample was fitted to a stainless steel sample holder with double sided carbon conductive tape. The equipment employed was a SPECS GmbH system equipped with a hemispherical energy analyzer PHOIBOS 150 9MCD. The X-ray source was non-monochromatic Mg (1253.6 eV) of 200 W and voltage of 12 kV. Firstly, samples were placed in the pre-treatment chamber at room temperature and degassed for several hours before being transferred to the analysis chamber. Pass energies were of 50 and 20 eV for acquiring respectively both survey and high resolution spectra.

2.12. X-ray diffraction

XRD qualitative measurements were carried out in a x'Pert Pro PANalytical polycrystal X-ray diffractometer, with a radiation of Cu-K_α ($\lambda = 1.5406$ Å, 40 mA). The acquisition time was 20 s for all samples, except for the completely assembled electrode, whose acquisition time was 1000 s for better resolution.

2.13. Scanning electron microscopy

The scanning electron microscopy was performed in a TM-1000 Hitachi Tabletop SEM apparatus. In order to control whether the coverage of the surface was homogeneous or not, several SEM pictures of different regions of the sample were taken.

3. Results

The chalcogenide used in this work was the polycrystalline β-In_2S_3, an orange-red powder material that was synthesized as in a previous work and its characterization has been already reported [15]. The In_2S_3 presented aggregates of size ranging from 50 nm to over 1 μm visible by SEM, a band-gap of 2.1 eV measured by total reflectance UV–vis spectroscopy, a specific area of 40.6 ± 0.3 m^2 per gram and an average pore width of 16.5 nm, yielding a total pore volume of 0.168 cm^3 per gram [15].

The In_2S_3 powder deposition on NiO-modified FTO electrodes was carried out using acetonitrile as dispersing solvent and spin coating as deposition technique. The resulting modified electrodes were further characterized through SEM, XPS and XRD.

Image characterization of the electrodes' coating was performed by SEM, Fig. 1. A smooth surface was obtained using spin coating as deposition technique, although some scattered aggregates were also observed on the surface of the electrodes. EDS X-ray characterization was available for the SEM measurements but yielded a mixture of signals from all the layers comprised in the electrode building, so we measured the surface composition by X-ray photoemission spectroscopy (XPS) aiming to find if the electrode surface is completely covered by the In_2S_3, Fig. 2.

XPS survey spectra were recorded for three different samples aiming to ensure the proper deposition of the semiconductors: a FTO-NiO modified electrode, a FTO-In_2S_3 electrode and a FTO-NiO-In_2S_3 electrode. For all of them the core spectra of S^{2p}, In^{3d}, Ni^{2p} and O^{1s} were accumulated, Fig. 2. The purpose of this analysis is measuring the surface quantitative proportions as well as ensuring the absence of exposed traces belonging to the inner layers. For the FTO-In_2S_3 electrode there are no traces of Ni^{2p} signals, whereas the signals of In^{3d} and S^{2p} are present, suggesting that the surface is fully covered with In_2S_3 and there is no FTO exposed. In fact, the S^{2p} and In^{3d} signals are significant only in the cases of FTO-NiO-In_2S_3 and FTO-In_2S_3 electrodes, while they do not appear in the FTO-NiO electrode, Fig. 2B and 2C respectively. The core spectra in Fig. 2D reveals the presence of Ni^{2p} in the cases of FTO-NiO-In_2S_3 and FTO-NiO electrodes, but the FTO-In_2S_3 electrode does not show peaks attributed to Ni^{2p}. O^{1s} peaks appear in the core spectra of the three samples, but FTO-In_2S_3 only shows a peak at 534 eV while FTO-NiO and FTO-NiO-In_2S_3 show two peaks at 532 and 534 eV, Fig. 2D. These divergences are attributed to the lack of NiO in the first case. Due to the surface analysis nature of the technique we can assume that either the edges of the electrode are included in the analysis spot recorded or the In_2S_3 coverage of the FTO-NiO electrode is incomplete so that the inner layers are exposed in some parts. It should be noted that the XPS were recorded prior to masking the electrodes with the epoxy dielectric paste, after masking the electrodes only the central spot window of 0.27 cm^2 is used.

The quantification of the XPS core signals for In and S shows that the amount of indium exposed on the surface is much higher (91 %) than the one expected from its stoichiometry (40 %). This disproportion may be a surface effect that is not present in the crystal cores. The same ratio was also observed for a FTO-In_2S_3 electrode, a freshly prepared FTO-NiO-In_2S_3 electrode and a used FTO-NiO-In_2S_3 electrode, indicating that the disproportion is not due to the electrode usage but generated during the XPS measurements or just a synthesis effect. A deconvolution of the In^{3d} signal for the FTO-NiO-In_2S_3 electrode was performed to find the contributions of In^{3+} and In^0, Fig. 2F. The resulting analysis shows that ~ 8 % of the surface In is in metallic form and ~ 92 % is In^{3+}, suggesting that some In nanoparticles formation or partial coverage occurs during the synthesis. In order to discard an incorrect synthesis, we performed also X-ray diffraction (XRD) to the modified electrodes.

The X-ray diffractogram (Fig. 3) shows that the peaks belonging to In_2S_3 polycrystalline powder before its modification correspond to those of polycrystalline β-In_2S_3 (the diffraction database 01–084-1385) and are reproduced on the FTO-NiO-In_2S_3 electrode. Besides, the peaks belonging to FTO and NiO at $2\Theta = 42, 44, 56, 70^\circ$ were also detected. From these XPS and XRD results it can be concluded that In_2S_3 is properly synthesized, although its surface has an excess of indium cations. Additionally, no traces of In^0 appear in the XRD, suggesting that the presence of In crystals is negligible. Finally, XRD allows calculating the crystal average size by using Scherrer's formula:

$$\tau = \frac{K\lambda}{\beta \bullet cos\theta} \quad (1)$$

Being τ the mean size of crystalline domains, λ the X-ray wavelength, K the shape factor, β the broaden of the highest peak at half of the maximum and θ the Bragg angle in radians. The calculation yields a τ value of 83.9 nm for both the powder of In_2S_3 and the In_2S_3 deposited onto the electrode [15]. It should be noted that XRD did not yield any diffraction peak belonging to metallic In^0. This result is in agreement with the hypothesis exposed earlier that the disproportion of In detected by XPS in the surface is not present in the bulk of the chalcogenide.

The electrodes modified with NiO and In_2S_3 were set into the photoelectrochemical cell for characterizing their performance. We analysed the chronoamperometric response at three different potentials: −0.6 V, −0.4 V and −0.2 V vs Ag/AgCl at pH 7. These potentials were selected to monitor the H_2 evolution in order that the current at −0.6 V shows the addition of the pure electrochemical reduction close to the onset potential plus the photoelectrochemical reduction of H_2, while the current at −0.2 V would show only the photoelectrochemical reduction of protons to H_2, as it is clearly above the thermodynamic value for proton reduction at neutral pH. A redox potential of −0.4 V was monitored as intermediate value between both processes.

A first characterization of FTO-NiO-In_2S_3 electrodes lacking Hase on its surface was performed, Fig. 4. The resulting currents yielded a significant difference between them in the time to stabilize the background current under dark conditions, which takes around 100 s when applying −0.2 V but it does not reach a plateau for the applied potentials of −0.4 V and −0.6 V. However, the average photocurrents are also much higher for the highly negative potentials ($i_{-0.6V}$ = -0.09 μA·cm^{-2}, $i_{-0.4V}$ = -0.09 μA·cm^{-2}) than for low negative potentials ($i_{-0.2V}$ = -0.04 μA·cm^{-2}). These results show the background currents expected for electrodes containing immobilized hydrogenase, as well as the success of the p-n junction strategy for these materials.

The incorporation of Hase on the surface of the chalcogenides was monitored in two different configurations: either physically adsorbed on its surface or covalently immobilized using aryldiazonium grafting strategy. One of the advantages of the covalent immobilization is that the enzyme gets oriented in an optimal way, with its active center facing

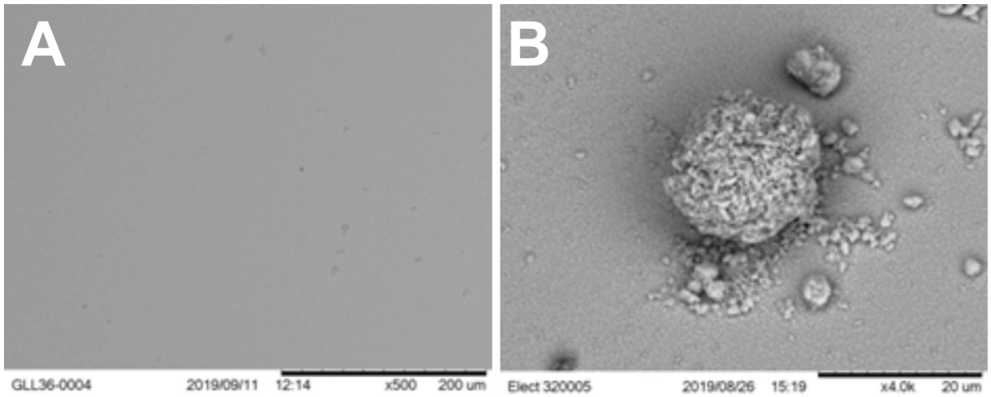

Fig. 1. Scanning Electron Microscopy images of the In_2S_3 layer deposited on the top of NiO-modified FTO electrodes using acetonitrile as solvent: (A) x500, (B) x4000.

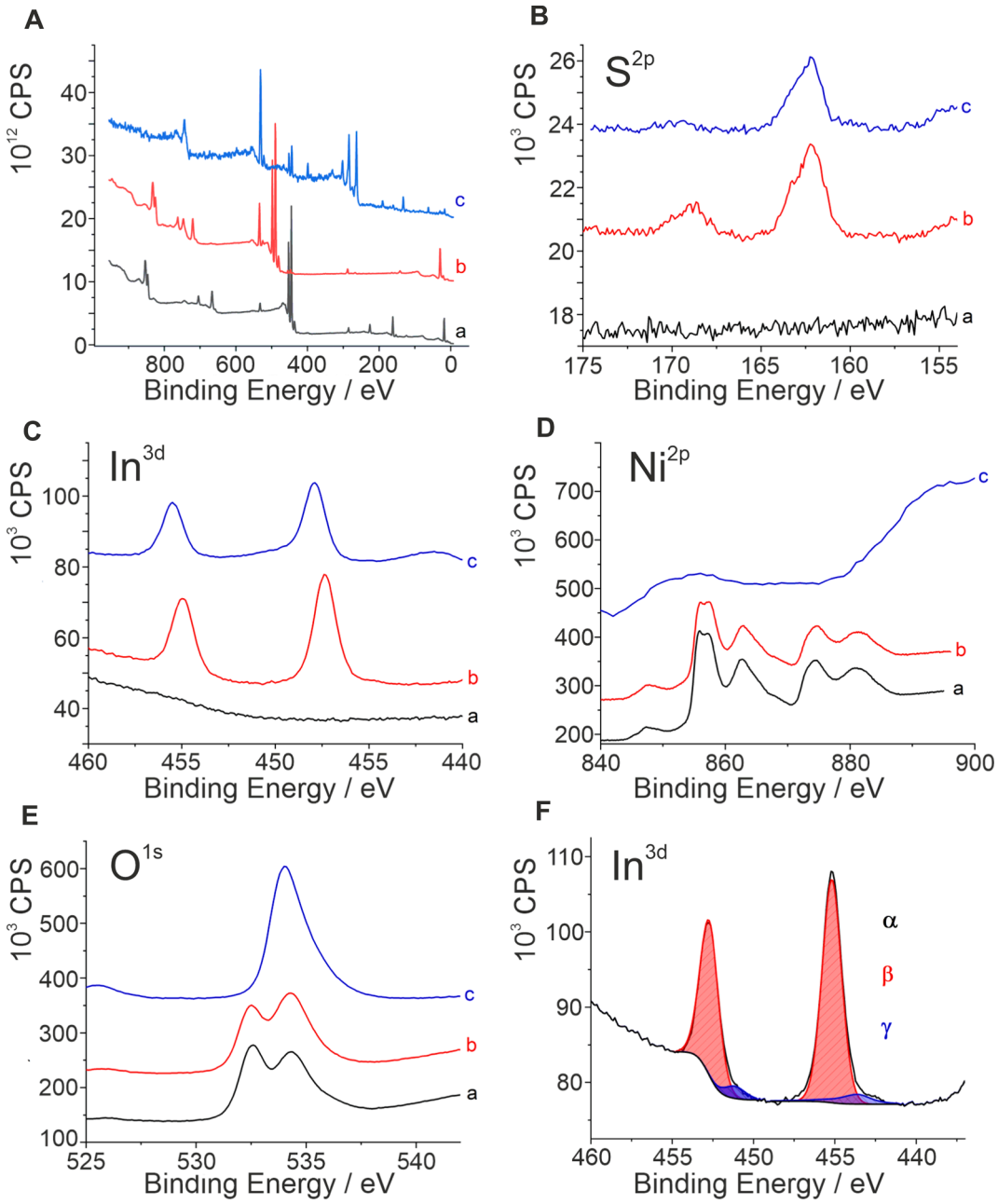

Fig. 2. XPS spectra of (a) FTO-NiO, (b) FTO-NiO-In_2S_3, (c) FTO-In_2S_3. (A) Survey spectra (B) Core spectra for sulfur, (C) core spectra for indium, (D) core spectra for nickel, (E) core spectra for oxygen, (F) Deconvolution of the indium signal for FTO-NiO-In_2S_3: (α) is the original spectra, (β) its deconvolution part for In^{3+}, (γ) the deconvolution for In^0.

the buffer and not the electrode. On the other hand, if the initial deposition of NBD is not correct, instead of a monolayer a multilayer can be formed, therefore increasing the distance from the electrode to the enzyme attached, critically reducing the efficiency of the whole system. Therefore, these methods have been compared because the physical adsorption yielded better results for In_2S_3-Hase photochemical H_2 production vs sacrificial electron donor [15], whereas covalent binding of laccase on FTO-In_2S_3 electrodes lead to improved O_2 evolution in photoelectrobiocatalytic experiments, [16,17]. Fig. 5 shows the different performance of Hase measured when physically absorbed or covalently linked.

The photocurrent increase provided by each electrode was measured by subtracting the current under dark conditions from that obtained upon irradiation. The photocurrent increase for the FTO-NiO-In_2S_3-Hase electrode with adsorbed enzyme was 1.43 μA·cm^{-2}, in contrast with the 1.20 μA·cm^{-2} obtained with the FTO-NiO-In_2S_3 electrode without the Hase, Fig. 5A. On the other hand, the FTO-NiO-In_2S_3-Hase electrode with covalently bound enzyme to the electrode yielded up to −2.38 μA·cm^{-2} as opposed to the highest −1.30 μA·cm^{-2} measured with that FTO-NiO-In_2S_3 electrode before adding the enzyme, Fig. 5B. While the immobilized enzyme boosts the photocurrent effect in all cases, the increase is higher for the covalent linked bioelectrode. This result is coherent since the covalent immobilization attaches the enzyme in an optimal way (orienting the active site towards the buffer bulk) to maximize the activity of the enzyme. In addition, this type of union improves the connectivity of the enzyme with the electrode and prevents further desorption towards the bulk of the buffer. The reproducibility study was carried on three different electrodes, which yielded a Δi of -1.7 ± 0.6 μA·cm^2 for the FTO-NiO-In_2S_3-Hase electrodes, whereas the FTO-NiO-In_2S_3 electrodes yielded a Δi of -1.1 ± 0.2 μA·cm^2.

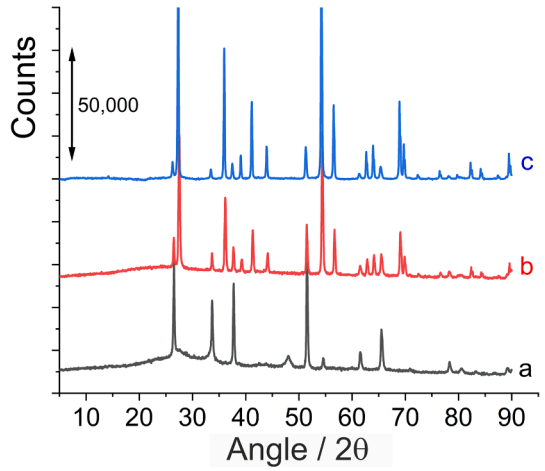

Fig. 3. X-ray diffractograms of (a) In_2S_3 *10, (b) FTO *10, (c) FTO-NiO-In_2S_3.

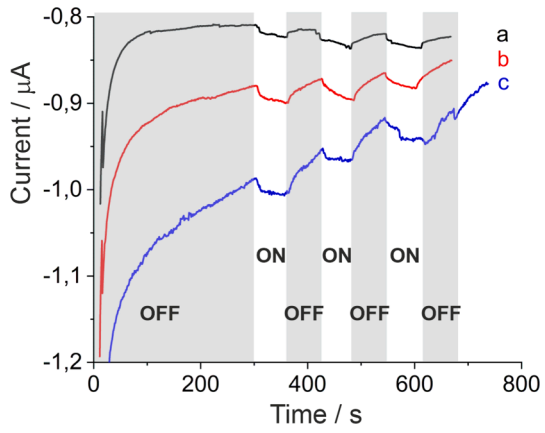

Fig. 4. Chronoamperometries of a FTO-NiO-In_2S_3 electrode at (a) −0.2 V, (b) −0.4 V, (c) −0.6 V vs Ag/AgCl (3 M NaCl). The light background marks the irradiation of the electrode with 1 Sun equivalent light power from a Xe arc lamp.

The effect of the p-n junction was analyzed by comparing the chronoamperometric response provided by an electrode modified with In_2S_3 and Hase but lacking the NiO layer with another electrode that contains the NiO layer, Fig. 6. Both electrodes were recorded at three different redox potentials, −0.2 V, −0.4 V and −0.6 V, while irradiating them intermittently during 2-min periods. The electrodes lacking the p-n junction gave no negative photocurrent or even a slight positive one, which cannot correspond to the reduction of protons to H_2 (Fig. 6 lines a2, a4, a6). On the other hand, the electrodes modified with the p-n junction and the Hase provided reduction photocurrents upon illumination (Fig. 6 lines b2, b4, b6). Even at a mild redox potential of −0.2 V the FTO-NiO-In_2S_3-Hase electrodes produced a significant negative photocurrent (Fig. 6 line b2) that proves the effect of photoactivation. At this redox potential a direct connection between the electrode and the enzyme would not yield any H_2 conversion.

Other results of hydrogenase-modified semiconductor electrodes operating under irradiating conditions have been reported [26–28]. The only work of them performed with the NiFeSe Hase we have used is the flagship work on photoelectrocatalytic production of H_2 achieved on a nanostructured inverse-opal TiO_2 built on a complex set of layers comprised in a full photoelectrochemical cell. The closest data reported of their photocurrents is in the order of -2 mA·cm^{-2} at a potential of + 0.5 vs RHE [26]; our p-n model shows -1.7 ± 0.6 μA·cm^2 at + 0.42 V vs RHE, which is −0.2 vs Ag/AgCl 3 M at pH 7. This work by Reisner and coworkers is a mature development containing nanostructured

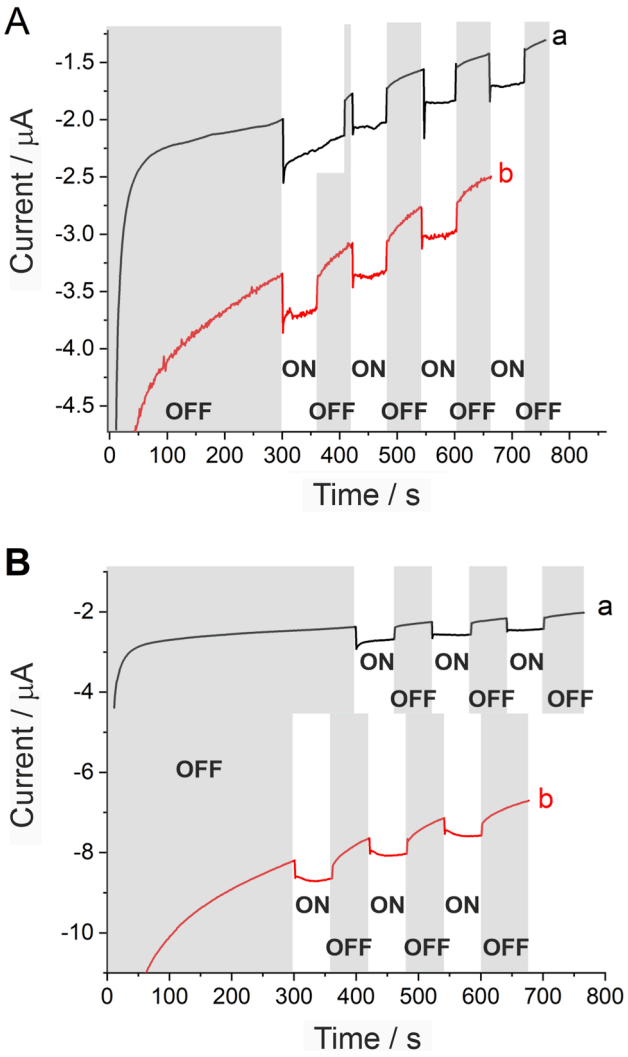

Fig. 5. Chronoamperometries recorded at −0.6 V vs Ag/AgCl 3 M of (A) FTO-NiO-In_2S_3 electrode (a) before and (b) after immobilization of Hase through absorption. (B) FTO-NiO-In_2S_3 electrode (a) before and (b) after immobilization of Hase through covalent linking.

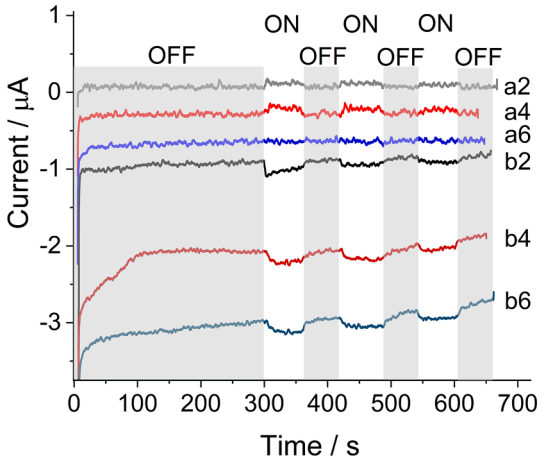

Fig. 6. Chronoamperometric response recorded for a FTO-In_2S_3-Hase electrode at (a2) −0.2 V, (a4) −0.4 V and (a6)-0.6 V and a FTO-NiO-In_2S_3-Hase at (b2) −0.2 V, (b4) −0.4 V and (b6)-0.6 V vs Ag/AgCl (3 M NaCl). The electrode was irradiated with a 1 Sun equivalent in the white zones of the graph.

electrodes and is out of the range for our proof-of-concept p-n junction system, as we only improve it by filtering out the UV radiation.

From the results obtained, it can be concluded that the inclusion of NiO as interstitial suitable p-type semiconductor allows the use of *n*-type semiconductors to produce H_2 from protons in absence of a sacrificial electron donor, by means of light, electricity and hydrogenase as co-catalyst.

4. Conclusions

The assistance of light energy is a key strategy to reduce the energy gap needed to produce green hydrogen by hydrogenase on an electrode. The absence of semiconductors combining all the requirements to favor this reaction can be overcome by the combination of several materials, particularly a *n*-type semiconductor with an adequate band gap to absorb visible light and band alignment to communicate with the Hase, and a p-type semiconductor to facilitate the electron replenishment from an electrode. It is shown in this work that the p-n junction boosts the performance of a hydrogenase, decreasing 400 mV the potential applied to obtain photocurrent for the proton reduction reaction. In contrast to other systems, like TiO_2, that cannot absorb visible light unless a photosensitizer is added, a p-n junction skips the use of such organic complexes. Future work will continue testing other semiconductor combinations.

Declaration of Competing Interest

The authors declare that they have no known competing financial interests or personal relationships that could have appeared to influence the work reported in this paper.

Data availability

Data will be made available on request.

Acknowledgements

G.L., A.I.J., J.C.C., A.L.D. and M.P. thank the ''Comunidad de Madrid'' for its support to the FotoArt-CM Project (S2018/NMT-4367) through the Program of R&D activities between research groups in Technologies 2018, co-financed by European Structural Funds. A.L.D. and M.P. thank MCIU/AEI/FEDER, EU for funding project RTI2018-095090-B-I00. A.M.C and I.A.C.P. thank the Fundação para a Ciência e Tecnologia PTDC/BII-BBF/2050/2020 grant, SFRH/BD/146475/2019 fellowship, MOSTMICRO-ITQB unit (UIDB/04612/2020 and UIDP/04612/2020) and LS4FUTURE Associated Laboratory (LA/P/0087/2020) for funding. J.F. and V.A. thank the support by the Agence Nationale de la Recherche (Labex ARCANE, CBH-EUR-GS, ANR-17-EURE-0003).

References

[1] B. Zhang, L. Sun, Artificial photosynthesis: opportunities and challenges of molecular catalysts, Chem. Soc. Rev. 48 (2019) 2216–2264, https://doi.org/10.1039/C8CS00897C.

[2] G. Segev, J. Kibsgaard, C. Hahn, Z.J. Xu, W.-H. Cheng, T.G. Deutsch, C. Xiang, J. Z. Zhang, L. Hammarström, D.G. Nocera, A.Z. Weber, P. Agbo, T. Hisatomi, F. E. Osterloh, K. Domen, F.F. Abdi, S. Haussener, D.J. Miller, S. Ardo, P.C. McIntyre, T. Hannappel, S. Hu, H. Atwater, J.M. Gregoire, M.Z. Ertem, I.D. Sharp, K.-S. Choi, J.S. Lee, O. Ishitani, J.W. Ager, R.R. Prabhakar, A.T. Bell, S.W. Boettcher, K. Vincent, K. Takanabe, V. Artero, R. Napier, B.R. Cuenya, M.T.M. Koper, R. Van De Krol, F. Houle, Solar fuels roadmap, J. Phys. D Appl. Phys. 55 (32) (2022) 323003, https://doi.org/10.1088/1361-6463/ac6f97.

[3] R.M. Navarro, M.A. Peña, J.L.G. Fierro, Hydrogen production reactions from carbon feedstocks: fossil fuels and biomass, Chem. Rev. 107 (2007) 3952–3991, https://doi.org/10.1021/cr0501994.

[4] A. Fujishima, K. Honda, Electrochemical photolysis of water at a semiconductor electrode, Nature 238 (1972) 37–38, https://doi.org/10.1038/238037a0.

[5] Q. Guo, C. Zhou, Z. Ma, X. Yang, Fundamentals of TiO_2 photocatalysis: concepts, mechanisms, and challenges, Adv. Mater. 31 (2019) 1901997, https://doi.org/10.1002/adma.201901997.

[6] V. Kumaravel, S. Mathew, J. Bartlett, S.C. Pillai, Photocatalytic hydrogen production using metal doped TiO2: a review of recent advances, Appl Catal B 244 (2019) 1021–1064, https://doi.org/10.1016/j.apcatb.2018.11.080.

[7] M. Grätzel, Recent Advances in Sensitized Mesoscopic Solar Cells, Acc. Chem. 42 (11) (2009) 1788–1798.

[8] A. Meng, L. Zhang, B. Cheng, J. Yu, Dual cocatalysts in TiO_2 photocatalysis, Adv. Mater. (2019) 1807660, https://doi.org/10.1002/adma.201807660.

[9] W. Lubitz, H. Ogata, O. Rüdiger, E. Reijerse, Hydrogenases, Chem. Rev. 114 (2014) 4081–4148, https://doi.org/10.1021/cr4005814.

[10] A.L. De Lacey, V.M. Fernández, M. Rousset, R. Cammack, Activation and inactivation of hydrogenase function and the catalytic cycle: spectroelectrochemical studies, Chem. Rev. 107 (2007) 4304–4330, https://doi.org/10.1021/cr0501947.

[11] M.A. Alonso-Lomillo, O. Rüdiger, A. Maroto-Valiente, M. Velez, I. Rodríguez-Ramos, F.J. Muñoz, V.M. Fernández, A.L. De Lacey, Hydrogenase-coated carbon nanotubes for efficient H2 oxidation, Nano Lett. 7 (2007) 1603–1608, https://doi.org/10.1021/nl070519u.

[12] E. Katz, A.L. de Lacey, V.M. Fernandez, Covalent binding of viologen to electrode surfaces coated with poly(acrylic acid) prepared by electropolymerization of acrylate ions, J. Electroanal. Chem. 358 (1993) 261–272, https://doi.org/10.1016/0022-0728(93)80443-L.

[13] E. Katz, A.L. de Lacey, J.L.G. Fierro, J.M. Palacios, V.M. Fernandez, Covalent binding of viologen to electrode surfaces coated with poly(acrylic acid) formed by electropolymerization of acrylate ions: I. Electrode preparation and characterization, J. Electroanal. Chem. 358 (1993) 247–259, https://doi.org/10.1016/0022-0728(93)80442-K.

[14] K.A. Brown, M.B. Wilker, M. Boehm, G. Dukovic, P.W. King, Characterization of photochemical processes for H2 production by CdS Nanorod–[FeFe] hydrogenase complexes, J. Am. Chem. Soc. 134 (2012) 5627–5636, https://doi.org/10.1021/ja2116348.

[15] C. Tapia, S. Zacarias, I.A.C. Pereira, J.C. Conesa, M. Pita, A.L. De Lacey, In situ determination of photobioproduction of H_2 by In_2S_3 -[NiFeSe] hydrogenase from *Desulfovibrio vulgaris* hildenborough using only visible light, ACS Catal. 6 (2016) 5691–5698, https://doi.org/10.1021/acscatal.6b01512.

[16] C. Tapia, S. Shleev, J.C. Conesa, A.L. De Lacey, M. Pita, Laccase-catalyzed bioelectrochemical oxidation of water assisted with visible light, ACS Catal. 7 (2017) 4881–4889, https://doi.org/10.1021/acscatal.7b01556.

[17] C. Jarne, L. Paul, J.C. Conesa, S. Shleev, A.L. De Lacey, M. Pita, Underpotential photoelectrooxidation of water by SnS_2 −laccase Co-catalysts on nanostructured electrodes with only visible-light irradiation, ChemElectroChem 6 (2019) 2755–2761, https://doi.org/10.1002/celc.201900360.

[18] J. Hu, B. Geng, J. Glowacki, S. Zhang, X. Yang, D. Pan, L. Shen, A biodegradable p-n junction sonosensitizer for tumor microenvironment regulating sonodynamic tumor therapy, Chem. Eng. J. 446 (2022), 137320, https://doi.org/10.1016/j.cej.2022.137320.

[19] K. Kim, H. Kim, E.-J. Jo, H. Jang, J. Park, G.Y. Jung, M.-G. Kim, Reactant/polymer hybrid films on p-n junction photodetectors for self-powered, non-invasive glucose biosensors, Biosens. Bioelectron. 175 (2021), 112855, https://doi.org/10.1016/j.bios.2020.112855.

[20] M. Zhao, J. Shang, H. Qu, R. Gao, H. Li, S. Chen, Fabrication of the Ni/ZnO/BiOI foam for the improved electrochemical biosensing performance to glucose, Anal. Chim. Acta 1095 (2020) 93–98, https://doi.org/10.1016/j.aca.2019.10.033.

[21] I. Yoo, S.S. Kalanur, H. Seo, A nanoscale p–n junction photoelectrode consisting of an NiOx layer on a TiO2/CdS nanorod core-shell structure for highly efficient solar water splitting, Appl Catal B 250 (2019) 200–212, https://doi.org/10.1016/j.apcatb.2019.02.063.

[22] M.C. Marques, C. Tapia, O. Gutiérrez-Sanz, A.R. Ramos, K.L. Keller, J.D. Wall, A. L. De Lacey, P.M. Matias, I.A.C. Pereira, The direct role of selenocysteine in [NiFeSe] hydrogenase maturation and catalysis, Nat. Chem. Biol. 13 (2017) 544–550, https://doi.org/10.1038/nchembio.2335.

[23] R. Lucena, I. Aguilera, P. Palacios, P. Wahnón, J.C. Conesa, Synthesis and spectral properties of nanocrystalline V-substituted In2S3, a novel material for more efficient use of solar radiation, Chem. Mater. 20 (2008) 5125–5127, https://doi.org/10.1021/cm801128b.

[24] R.L.Z. Hoye, L.C. Lee, R.C. Kurchin, T.N. Huq, K.H.L. Zhang, M. Sponseller, L. Nienhaus, R.E. Brandt, J. Jean, J.A. Polizzotti, A. Kursumović, M.G. Bawendi, V. Bulović, V. Stevanović, T. Buonassisi, J.L. MacManus-Driscoll, Strongly enhanced photovoltaic performance and defect physics of air-stable bismuth oxyiodide (BiOI), Adv. Mater. 29 (2017) 1702176, https://doi.org/10.1002/adma.201702176.

[25] P. Allongue, M. Delamar, B. Desbat, O. Fagebaume, R. Hitmi, J. Pinson, J.-M. Savéant, Covalent modification of carbon surfaces by aryl radicals generated from the electrochemical reduction of diazonium salts, J. Am. Chem. Soc. 119 (1997) 201–207, https://doi.org/10.1021/ja963354s.

[26] E. Edwardes Moore, V. Andrei, S. Zacarias, I.A.C. Pereira, E. Reisner, Integration of a hydrogenase in a lead halide perovskite photoelectrode for tandem solar water

splitting, ACS Energy Lett. 5 (2020) 232–237, https://doi.org/10.1021/acsenergylett.9b02437.

[27] Y. Zhao, N.C. Anderson, M.W. Ratzloff, D.W. Mulder, K. Zhu, J.A. Turner, N. R. Neale, P.W. King, H.M. Branz, Proton reduction using a hydrogenase-modified nanoporous black silicon photoelectrode, ACS Appl. Mater. Interfaces 8 (2016) 14481–14487, https://doi.org/10.1021/acsami.6b00189.

[28] L. Tian, B. Németh, G. Berggren, H. Tian, Hydrogen evolution by a photoelectrochemical cell based on a Cu2O-ZnO-[FeFe] hydrogenase electrode, J. Photochem. Photobiol. A Chem. 366 (2018) 27–33, https://doi.org/10.1016/j.jphotochem.2018.01.035.